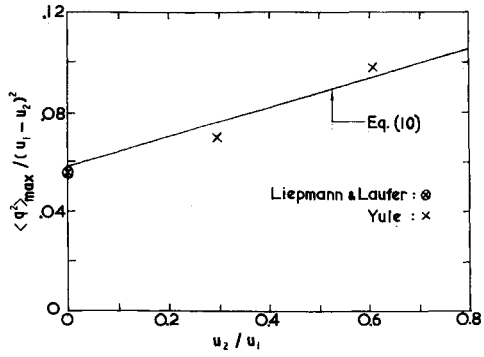

Fig. 3 Variation of dimensionless peak turbulence intensity with free-stream velocity ratio.

Agreement with experiment is poor (Fig. 1) however this discrepancy is explained when the eddy viscosity assumption is written in a more logical form. The hypothesis implies a dominating gradient diffusion process and such a process would be controlled by the energy containing turbulence. The eddy viscosity should be dependent upon this turbulence and not necessarily upon the local scales of the mean velocity distribution, thus a better choice of the velocity scale is the rms peak turbulence intensity $\langle q^2\rangle^{\frac{1}{2}}_{max}$. However it may be expected that the local turbulence dictates the width of the mixing layer and indeed measurements[3] show that $b = Ax/\sigma$, from Eq. (4), gives good correlation between the turbulence length scales at different velocity ratios. The new eddy-viscosity assumption is

$$\nu_T = K_\gamma b\langle q^2\rangle^{\frac{1}{2}}_{max} \tag{7}$$

and with this assumption σ is [c.f. Eq. (2)]

$$\sigma = \tfrac{1}{2}\{(K_\gamma db/dx)\langle q^2\rangle^{\frac{1}{2}}_{max}/(u_1+u_2)\}^{-\frac{1}{2}} \tag{8}$$

Equation (4) and Eq. (8) give

$$\sigma = (4K_\gamma A)^{-1}\{(u_1+u_2)/(u_1-u_2)\}\{\langle q^2\rangle^{\frac{1}{2}}_{max}/(u_1-u_2)\}^{-1} \tag{9}$$

The variation of $\langle q^2\rangle^{\frac{1}{2}}_{max}/(u_1-u_2)$ which is implied by the σ distribution is given by Eq. (3) and Eq. (9)

$$\langle q^2\rangle_{max}/(u_1-u_2)^2 = (4K_\gamma A\sigma_0)^{-2}(1+u_2/u_1) \tag{10}$$

Table 1 Experimental mixing layer parameters

Source	u_2/u_1	σ	$\langle q^2\rangle_{max}/(u_1-u_2)^2$	$K_\gamma A$	$K_G A$
Wygnanski and Fiedler[6]	0	9	0.071	0.104	0.028
Liepmann and Laufer[5]	0	11	0.056	0.096	0.023
Yule[3]	0.30	19	0.069	0.094	0.024
Yule[3]	0.61	36	0.098	0.092	0.029

The results in Table 1 were corrected for tangential cooling effects and for Liepmann and Laufer's results it was assumed, following Townsend,[8] $\langle q^2\rangle_{max} = \frac{3}{2}(\langle(u')^2\rangle_{max}+\langle(v')^2\rangle_{max})$. This gives agreement to within 4% for the author's measurements. Wygnanski attributed his lower value of σ (i.e., a faster rate of spread) to the use of a trip wire at the separating plate edge and this explanation correlates with the higher turbulence levels observed. The remaining data agree with the new constant eddy-viscosity hypothesis, i.e. $K_\gamma A = 0.094 \pm 0.002$ but the coefficient $K_G A$ varies by 15%.

Measurements of $\langle q^2\rangle_{max}/(u_1-u_2)^2$ are compared with Eq. (10) in Fig. 3 and the agreement is encouraging. The increase in $\langle q^2\rangle_{max}/(u_1-u_2)^2$ with u_2/u_1 is associated with changes in the structure of the turbulence. This has important repercussions when the problem of jet noise is under consideration and it is a phenomenon worthy of further investigation.

References

[1] Görtler, H., "Berechnung von Aufgaben der Frein Turbulenz auf Grund eines Neuen Nahrungsansatzes," *Zeitschrift fuer Ansewandte Mathematik und Mechanik*, Vol. 22, No. 5, 1942, pp. 244–254.

[2] Miles, J. B. and Shih, J. S., "Similarity Parameter for Two-Stream Turbulent Jet-Mixing Region," *AIAA Journal*, Vol. 6, No. 7, July 1968, pp. 1429–1430.

[3] Yule, A. J., "Experimental and Analytical Investigations of Two Types of Turbulent Mixing Flow," Ph.D. thesis, Oct. 1969, Dept. of the Mechanics of Fluids, Univ. of Manchester, Manchester, England, Chap. 2.

[4] Yule, A. J., "Two-Dimensional Self-Preserving Turbulent Mixing Layers at Different Free Stream Velocity Ratios," R. & M. 3683, 1971, Aeronautical Research Council, London, England.

[5] Liepmann, H. H. and Laufer, J., "Investigations of Free Turbulent Mixing," TN 1257, 1947, NACA.

[6] Wygnanski, I. and Fiedler, H. E., "The Two-Dimensional Mixing Region," *Journal of Fluid Mechanics*, Vol. 41, Part 2, 1970, pp. 327–361.

[7] Nash, J. F., "The Effect of an Initial Boundary Layer on the Development of a Turbulent Free Shear Layer," CP 682, 1963, Aeronautical Research Council, London, England.

[8] Townsend, A. A., *The Structure of Turbulent Shear Flow*, University Press, Cambridge, England, 1956, p. 181.

Transient Gas Concentration Measurements Utilizing Laser Raman Spectroscopy

D. L. HARTLEY*
Sandia Laboratories, Livermore, Calif.

Introduction

A NUMBER of problems in the field of gas-dynamics require sophisticated techniques for measuring the pressure, temperature, and specie concentrations of unsteady, multispecie gas flows. Such problems as the study of reacting boundary layers, gas combustion systems, and expanding jets are among the many applications of these techniques. Although methods for measuring pressure and temperature of these flows have been developed, little has been done to develop an adaptable means of measuring the concentration of one gas specie in the presence of a dissimilar gas.

Recently, the technique of applying the laser Raman effect, whereby individual gaseous species are identified by a wavelength shift in scattered light, has developed into a usable engineering diagnostic tool. The inherent problem with the Raman scattering technique is the very small Raman scattering cross section of gases. Thus, even recent work with gases has involved long-time integration to attain usable signals.[1-4] The advent of the high-power pulsed lasers, however, has allowed single-pulse Raman spectroscopy.[5-8] Widhopf and Lederman[7] demonstrated, with a single pulse ruby laser, that gaseous concentrations could be measured from a lower limit of a few torr partial pressure.

In the system described in this paper,[8] a gas is injected into a spherical chamber which contains an originally quiescent, dissimilar gas. A multiple-pulsed nitrogen laser with single-pulse

Presented as Paper 71-286 at the AIAA 6th Aerodynamic Testing Conference, Albuquerque, New Mexico, March 10–12, 1971; submitted April 2, 1971; revision received December 2, 1971. This work was supported by the United States Atomic Energy Commission, contract number AT-(29-1)-789.

Index category: Jets, Wakes, and Viscid-Inviscid Flow Interactions.

* Staff Member, Aerothermodynamics Division.

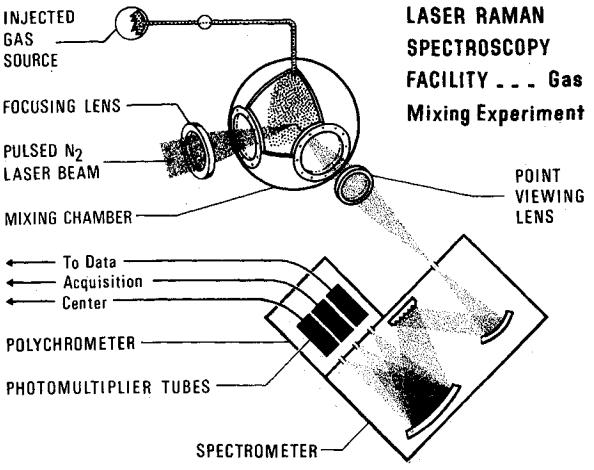

Fig. 1 Optical system used in laser Raman spectroscopy facility.

resolution is used to obtain a record of the resulting gas-mixing dynamics from a 1-mm-diam spot within the mixing gases.

Optical Design

The optical system employed in the current study is illustrated in Fig. 1. The illuminating source is a pulsed nitrogen laser which emits a 10-nanosec, 100-kw pulse at a rate of up to 100 pulses per sec. The output is at 3371 Å.

The mixing chamber is a spherical cavity with a 6-in. internal diameter. To reduce internal reflections, the vessel was plated with copper which was then oxidized to give a flat black surface. There are four sapphire windows in the chamber on orthogonal axes which allow transmission of the UV laser light.

Electronics

The Raman signal from each photomultiplier tube is integrated by a Lecroy 227 gated integrator. Both the laser and the integrator are synchronized and controlled by a central logic system; the controller pulses the laser and, following an adjustable time differential of up to 1 μsec, turns on the integrator. A 50-nanosec on-time is allowed for the integrator to catch the 10-nanosec photomultiplier output signal. The integrator is then turned off by the controller. However, the readout maintains a constant output which corresponds to the integral peak. Prior to each subsequent laser pulse, the integrator receives a re-zero signal from the controller.

The output of the integrator is electronically filtered to remove some of the statistical fluctuations and the high-frequency re-zero pulse. Both the filtered and the unfiltered signals are recorded along with the mixing chamber pressure and the driver pressure on a strip chart recorder.

Experimental Results

Both static and dynamic measurements were taken to verify the capabilities of the Raman scattering technique.

A. Static Measurements

Since the number of photons scattered at the Raman frequency is directly proportional to the number of scattering centers (i.e., to the density of the gas particles), one would expect the Raman signal to be a linear function of the gas density. This was verified by filling the mixing chamber with pure nitrogen to each of a series of fixed pressures, pulsing the laser, and recording the Raman signal amplitudes. The results of the measurements are shown in Fig. 2.

Helium was then added to the nitrogen at a series of static pressure levels to determine its effect on the nitrogen Raman signal. As Fig. 2 shows, the added helium had no effect on the intensity of the scattered light. Thus, the measurements verified that the nitrogen Raman signal amplitude is a function only of the nitrogen partial pressure.

The results obtained by adding helium to the nitrogen also proved that the collected signal was entirely made up of the Raman wavelength and was not affected by the large Rayleigh background. Wavelength isolation was also investigated by scanning the spectrometer through a spectrum from 3000 Å to 4000 Å. The Rayleigh signal at 3371 Å was about 10% as large as the nitrogen Raman signal at 3658 Å. The reduced Rayleigh signal is a result of the long-pass filter used on the spectrometer input. Another signal, also about 10% as large as the nitrogen Raman signal, and corresponding to the secondary emission line present in the laser output, was observed at 3576 Å. The remainder of the spectrum had no detectable signal.

Signals received at the lower concentration levels were very noisy. Calculations show that at 10 psi of nitrogen the system is collecting only about 16 photons of scattered light per pulse. By using the specified quantum efficiency of the RCA 8850 photocathode of 30%, one can calculate that only 5 photoelectrons are generated per pulse. Thus, one should expect a statistical fluctuation on the number of photoelectrons of $\pm(5)^{1/2}$, or an uncertainty of $\pm 40\%$. This effect was observed in the results and several pulses were integrated to obtain an accurate calibration at the lower pressure levels. At higher pressure levels, the statistical fluctuation diminishes to 10% at 200 psi and to 3% at 2000 psi. Reduced statistical noise could be attained by working at high pressures, by integrating more than one pulse, or by using a more powerful laser source.

B. Dynamic Measurements

A series of gas-mixing experiments was performed to illustrate that the laser Raman system could be used to obtain rapidly changing concentration measurements. In these experiments, a measured amount of nitrogen was injected from a 3000-psi piston-driven cylinder into a mixing chamber which contained helium at a known pressure. Raman scattered light was monitored from a 1 mm-diam sample volume halfway across the mixing chamber from the orifice. Nitrogen concentration recordings were obtained from several locations within the mixing chamber. Typical results obtained when 65 cm^3 of nitrogen at 3000 psi was injected into a container filled with 100 psi of helium are presented in Fig. 3. The final equilibrium pressure in the mixing chamber was about 175 psi.

The bottom curve corresponds to the nitrogen concentration profile when the mixing chamber pressure has increased by one third of its final pressure change. The subsequent curves correspond to one half, two thirds, and complete pressure

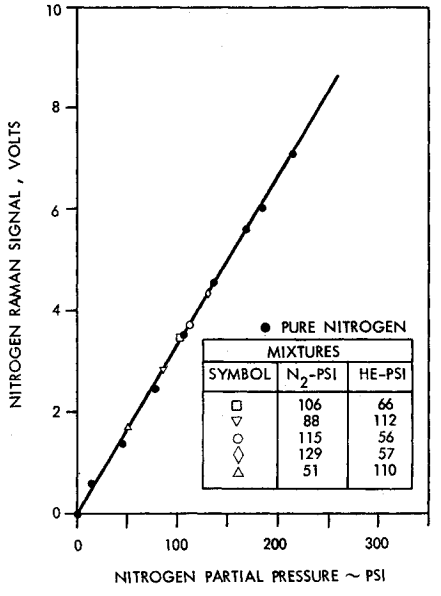

Fig. 2 Static measurement of Raman Stokes intensity of nitrogen (N_2) as a function of pressure.

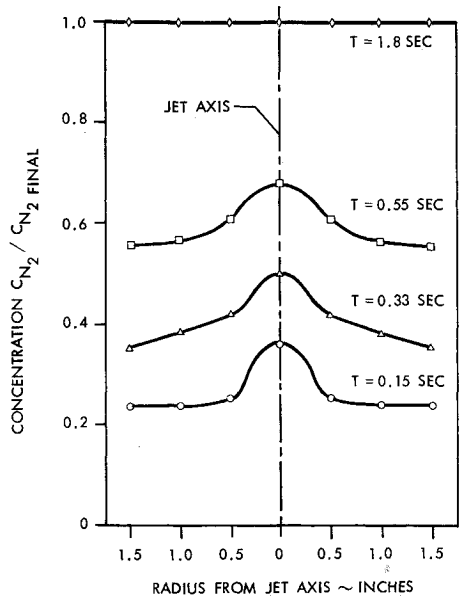

Fig. 3 Nitrogen concentration profiles for direct injection into helium.

equilibrium. These results indicate that by the time all the gas had been transferred to the mixing chamber (approximately 1.8 sec), the nitrogen and helium were uniformly mixed.

Conclusions

The experimental results have verified the linear behavior of the intensity of Raman scattered light as a function of specie concentration. It can be concluded that the technique is capable of identifying and measuring concentrations of individual gaseous species in a mixture during a single 10-nanosec sampling time. By repeating the sampling at the laser rate of 100 pulses per sec, it is possible to monitor a dynamic gas flow situation. For the case of 65 cm^3 of nitrogen at 3000 psi injected into a spherical mixing chamber containing 100 psi of helium, results obtained using the Raman scattering technique illustrate the rapid mixing which is occurring in the vessel. The proven merit of this facility has encouraged the extension of the technique to the study of general gas mixing problems, evaluation of transport properties, and the study of high-pressure, real gas effects.

References

[1] Herzberg, G., *Molecular Spectra and Molecular Structure,* Vol. 1, Van Nostrand, Princeton, N.J., 1967, pp. 61–65.

[2] Weber, A., Porto, S. P., Cheesman, L. E., and Barrett, J. J., "High Resolutions Raman Spectroscopy of Gases with cw-Laser Excitation," *Journal of the Optical Society of America,* Vol. 57, No. 1, Jan. 1967, pp. 19–27.

[3] Leonard, D. A., "Observation of Raman Scattering from the Atmosphere Using a Pulsed Nitrogen Ultraviolet Laser," *Nature,* Vol. 216, No. 5111, Oct. 14, 1967, pp. 142–143.

[4] Klainer, S. M., Hirschfeld, T., and Schildkrant, E. R., *The Detection of Toxic Contaminants in the Atmosphere Using Single Ended Remote Raman Spectrometric Techniques,* Meeting of the Central States Section of the Combustion Institute, Houston, Texas, April 1970.

[5] Delhaye, M., "Conventional Laser Raman Spectroscopy and Ultra-Fast Spectra," *Fourth Conference on Molecular Spectroscopy,* The Institute of Petroleum, Adlard & Son Ltd., Dorking, Great Britain, 1968, pp. 275–280.

[6] Markstein, G. and Daiber, J., *Turbulent Jet Mixing,* CAL TR CM-2637-A-1, Feb. 1970, Cornell Aeronautical Lab., Buffalo, N.Y.

[7] Widhopf, G. F. and Lederman, S., "Specie Concentration Measurements Utilizing Raman Scattering of a Laser Beam," *AIAA Journal,* Vol. 9, No. 2, Feb. 1971, pp. 309–316.

[8] Hartley, D. L., "Unsteady Multispecie Gas Mixture Concentration Measurements Using Laser Raman Scattering," *Proceedings of SPIE 15th Technical Symposium,* Anaheim, Calif., Sept. 1970, p. 115.

Solution of Unsteady Flow of Power Law Fluids

TOMMY Y. W. CHEN* AND DAVID E. WOLLERSHEIM†
University of Missouri, Columbia, Mo.

Nomenclature

B = constant, Eqs. (15) and (21)
C = constant of integration
C_f = coefficient of skin friction
$F(\eta)$ = dimensionless velocity distribution for ISP
$f'(\eta)$ = dimensionless velocity distribution for ISF
K = flow consistency index
N = flow behavior index, or power law fluid index
Re_t = Reynolds number in terms of time
t = time
u = fluid velocity in x-axis direction
U_0 = constant velocity in x-axis direction
x = horizontal coordinate
y = distance from the wall, vertical coordinate
μ = absolute viscosity
ρ = fluid density
ϕ = defined in Eqs. (4) and (6)
τ_{xy} = xy component of shear stress
τ_0 = shear stress at wall
τ_0^* = dimensionless shear stress at wall
δ^* = dimensionless boundary layer thickness
η = similarity parameter defined in Eq. (3a)
ξ = coordinate transformation variable

Subscript

∞ = undisturbed fluid

Introduction

IMPULSIVELY started flow of any power law fluid over a stationary and infinite plate, or an impulsively started plate in any power law fluid moving in its own plane with a constant velocity has been studied analytically.[1–3] Unfortunately, the solutions which can be integrated in closed form were derived only for pseudoplastic and Newtonian fluids (power law fluid index $N \leq 1$). Recently, Rott[4] presented a solution for an impulsively started plate in a dilatant fluid.

This Note presents the solutions for all power law fluids for both an impulsively started plate and flow cases, including the velocity distribution near the plate, shear stress near the wall, and boundary-layer thickness. The solutions are shown in expressions which can be integrated in closed form. They appear simpler than but are consistent with the results from the previously cited references.

Impulsively Started Plate (ISP)

For an impulsively started plate moving with a constant velocity U_0 in a power law fluid, the velocity gradient is everywhere negative. It is conventional to have a positive shear stress expression for any power law fluid

$$\tau_{xy} = -K\,|\partial u/\partial y|^{N-1}\,\partial u/\partial y \tag{1}$$

The equation of motion for the system becomes

$$\rho\,\partial u/\partial t = -\partial \tau_{xy}/\partial y = K\,\partial/\partial y\,(|\partial u/\partial y|^{N-1}\,\partial u/\partial y) \tag{2}$$

Employing the similarity transformation, let

$$\eta = y\phi(t) \quad \text{and} \quad F(\eta) = u/U_0 \tag{3a, b}$$

where $\phi(t)$ is a function to be found. Substituting Eqs. (3a, b) into Eq. (2), we find

Received May 18, 1971; revision received September 14, 1971.
Index category: Boundary Layer and Convective Heat Transfer—Laminar.

* Research Assistant, Department of Mechanical and Aerospace Engineering. Associate Member AIAA.
† Associate Professor, Department of Mechanical and Aerospace Engineering. Member AIAA.